The Primordial Inflation Polarization Explorer (PIPER)

Alan Kogut[a], Peter A. R. Ade[b], Dominic Benford[a], Charles L. Bennett[c], David T. Chuss[a], Jessie L. Dotson[d], Joseph R. Eimer[c], Dale J. Fixsen[a], Mark Halpern[e], Gene Hilton[f], James Hinderks[a], Gary F. Hinshaw[e], Kent Irwin[f], Christine Jhabvala[g], Brad Johnson[h], Justin Lazear[c], Luke Lowe[a], Timothy Miller[g], Paul Mirel[a], S. Harvey Moseley[a], Samelys Rodriguez[a], Elmer Sharp[a], Johannes G. Staguhn[a], Carole E. Tucker[b], Amy Weston[a], and Edward J. Wollack[a]

[a]Code 665, NASA Goddard Space Flight Center, Greenbelt, MD USA 20771;
[b]Cardiff University, Cardiff, Wales CF103XQ, UK;
[c]Johns Hopkins University, 3400 N. Charles St., Baltimore, MD USA 21218;
[d]NASA Ames Research Center, Moffett Field, CA, USA 94035;
[e]Dept. of Physics & Astronomy, University of British Columbia, Vancouver, BC, Canada, V6T 1Z1;
[f]Mailcode 817.03 National Institute for Standards and Technology, Boulder, CO USA 80305;
[g]Code 553, NASA Goddard Space Flight Center, Greenbelt, MD USA 20771;
[h]Columbia University, New York, NY USA 10027

ABSTRACT

The Primordial Inflation Polarization Explorer (PIPER) is a balloon-borne instrument to measure the gravitational-wave signature of primordial inflation through its distinctive imprint on the polarization of the cosmic microwave background. PIPER combines cold (1.5 K) optics, 5120 bolometric detectors, and rapid polarization modulation using VPM grids to achieve both high sensitivity and excellent control of systematic errors. A series of flights alternating between northern and southern hemisphere launch sites will produce maps in Stokes I, Q, U, and V parameters at frequencies 200, 270, 350, and 600 GHz (wavelengths 1500, 1100, 850, and 500 μm) covering 85% of the sky. The high sky coverage allows measurement of the primordial B-mode signal in the 'reionization bump" at multipole moments $\ell < 10$ where the primordial signal may best be distinguished from the cosmological lensing foreground. We describe the PIPER instrument and discuss the current status and expected science returns from the mission.

Keywords: polarimeter, cosmic microwave background, bolometer

1. INTRODUCTION

A central principle in modern cosmology is the concept of inflation, which posits a period of exponential expansion in the early universe. The many e-foldings of the scale size during inflation force the geometry of space-time to asymptotic flatness while dilating quantum fluctuations in the inflaton potential to the macroscopic scales responsible for seeding large-scale structure in the universe. Inflation provides a simple, elegant solution to multiple problems in cosmology, but it relies on extrapolation of physics to energies more than 12 orders of magnitude beyond those accessible to particle accelerators.

A critical test of inflation is its prediction of a background of gravitational waves. If inflation is responsible for the observed temperature fluctuations, gravitational waves are expected to exist: just as quantum fluctuations in the inflaton field generate a background of density perturbations, fluctuations in the space-time *metric* during inflation generate a stochastic background of gravitational waves. In the simplest inflationary models, the amplitude of this background depends on the inflationary potential

$$V^{1/4} = 1.06 \times 10^{16}\ \mathrm{GeV} \left(\frac{r}{0.01}\right)^{1/4} \quad (1)$$

Send correspondence to: Alan.J.Kogut@nasa.gov; telephone 1 301 286 0853

Millimeter, Submillimeter, and Far-Infrared Detectors and Instrumentation for Astronomy VI,
edited by Wayne S. Holland, Jonas Zmuidzinas, Proc. of SPIE Vol. 8452,
84521J © 2012 SPIE · CCC code: 0277-786X/12/$18 · doi: 10.1117/12.925204

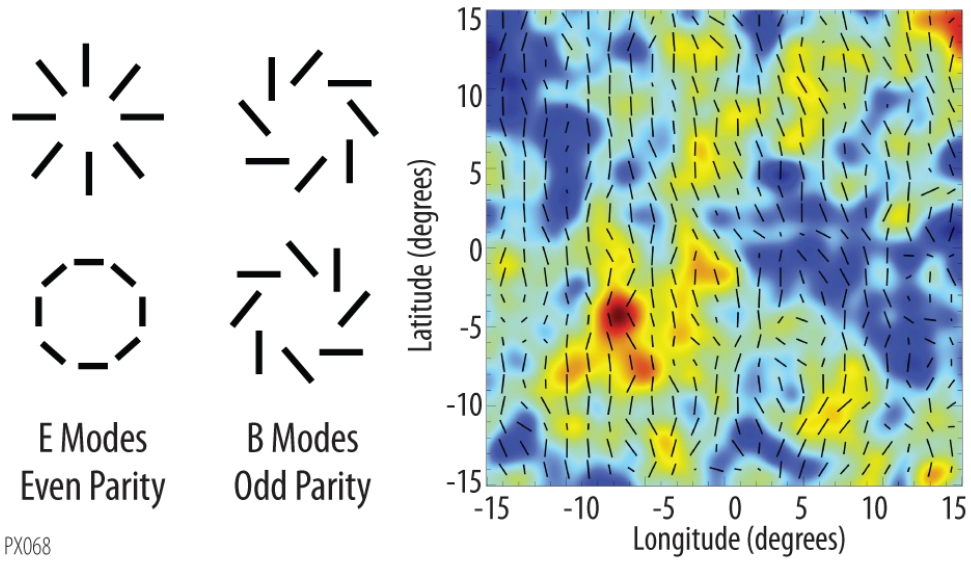

Figure 1. Simulated sky map showing CMB anisotropy (color) and polarization over a $30^\circ \times 30^\circ$ patch of sky. The polarization pattern can be decomposed into even-parity E-modes and odd-parity B-modes. Only gravitational waves can produce a B-mode signal in the CMB on large angular scales.

where r is the power ratio of gravitational waves to density fluctuations.

Polarization of the cosmic microwave background (CMB) provides a direct test of inflationary physics. CMB polarization results from Thomson scattering of CMB photons by free electrons. A quadrupolar anisotropy in the radiation incident on each electron creates a net polarization in the scattered radiation. There are only two possible sources for such a quadrupole: either an intrinsic temperature anisotropy or the differential redshift caused by a propagating gravitational wave. The two cases can be distinguished by their different spatial signatures (Figure 1). Temperature perturbations are scalar quantities; their polarization signal must therefore be curl-free. Gravitational waves, however, are tensor perturbations whose polarization includes both gradient and curl components. In analogy to electromagnetism, the scalar and curl components are often called "E" and "B" modes. Only gravitational waves induce a curl component on large angular scales: detection of a B-mode signal in the CMB polarization field is recognized as a "smoking gun" signature of inflation, testing physics at energies inaccessible through any other means.[1–8]

Figure 2 shows the CMB polarization as a function of angular scale. At the degree angular scales characteristic of the horizon at decoupling, the unpolarized temperature anisotropy is typically 80 μK. These fluctuations in turn generate E-mode polarization, which at amplitude $\sim$3 μK is only a few percent of the temperature fluctuations. The B-mode amplitude from gravitational waves is unknown. Recent WMAP results suggest values $0.01 < r < 0.1$ for large-field inflation models, corresponding to Grand Unification energy scales or polarization amplitudes in the range 30 to 100 nK.[9] Signals at this amplitude could be detected by a dedicated polarimeter, providing a direct, model-independent measurement of the energy scale of inflation.

Detecting the gravitational-wave signature will be difficult. As recognized in multiple reports,[10–12] there are three fundamental challenges:

- **Sensitivity** The gravitational-wave signal is faint compared to the fundamental sensitivity limit imposed by photon arrival statistics. Even noiseless detectors suffer from this photon-counting limit; the only solution is to collect more photons.
- **Foregrounds** The gravitational-wave signal is faint compared to the polarized Galactic synchrotron and dust foregrounds. Separating CMB from foreground emission based on their different frequency spectra requires multiple frequency channels.

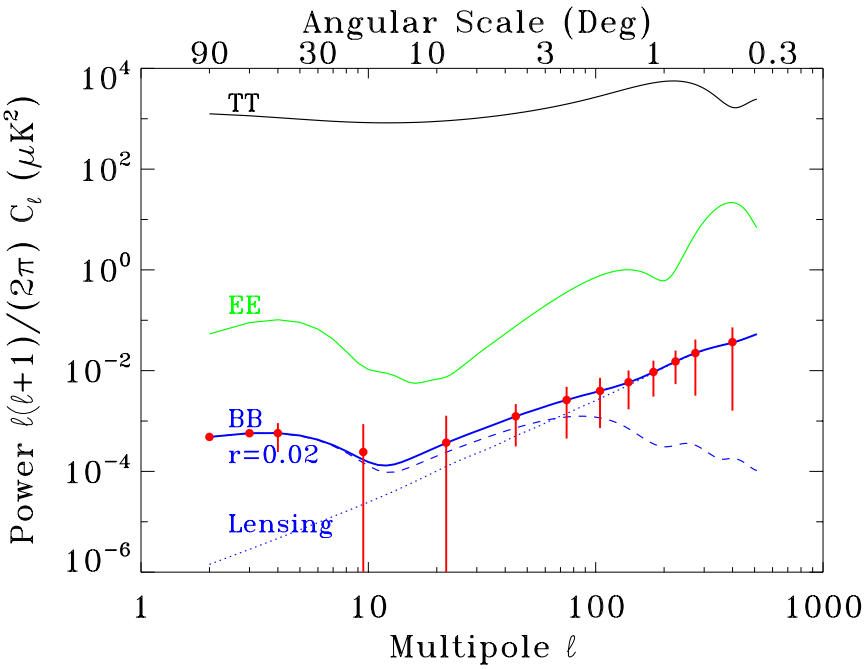

Figure 2. Angular power spectra for unpolarized, E-mode, and B-mode polarization in the cosmic microwave background. Filled points and error bars show the PIPER sensitivity to the B-mode power spectrum with amplitude $r = 0.02$. PIPER has the sensitivity and sky coverage required to detect the primordial signal within the "reionization bump" at large angular scales where it may best be distinguished from the competing lensing signal.

- **Systematic Errors** The gravitational-wave signal is faint compared to both the unpolarized CMB anisotropy and the dominant E-mode polarization. Accurate measurement of the B-mode polarization requires strict control of instrumental effects that could alias these brighter signals into a false B-mode detection.

Satisfying the simultaneous requirements of sensitivity, foreground discrimination, and immunity to systematic errors presents a technological challenge. Cosmological foregrounds present an additional operational challenge. Gravitational lensing by the matter distribution between the surface of last scattering at $z \approx 1090$ and the observer today produces a shear field, shifting a fraction of the dominant E-mode polarization into a B-mode lensing signal (dotted line in Figure 2). This lensing foreground dominates the inflationary signal on small angular scales. On intermediate scales of a few degrees, the lensing foreground has a similar power spectrum as the primordial signal and (for primordial amplitude near the expected value $r \sim 0.02$) a comparable amplitude.

Distinguishing the primordial signal form the lensing foreground requires mapping the polarization over a significant fraction of the sky. Inflation produces a stochastic background of gravitational waves, which source CMB polarization via Thomson scattering. Multiple scatterings, however, erase information from any previous scattering. The B-mode power spectrum is thus modulated by the ionization history of the universe, with two prominent peaks corresponding to changes in the ionization fraction of the early universe. The last scattering at recombination (redshift $z \approx 1090$) as the universe shifts from an ionized to a neutral medium produces a B-mode peak at angular scales of a few degrees. Re-ionization of the universe at redshift $z \approx 10$ scatters a fraction of the CMB photons to produce a second B-mode peak on large angular scales. This "reionization bump" at angular scales $\theta > 30°$ is an important discriminant for the primordial signal, allowing clean separation of the primordial signal from the lensing foreground.

This paper describes an instrument designed to characterize primordial inflation through its distinctive signature in the polarization of the cosmic microwave background. The Primordial Inflation Polarization Explorer

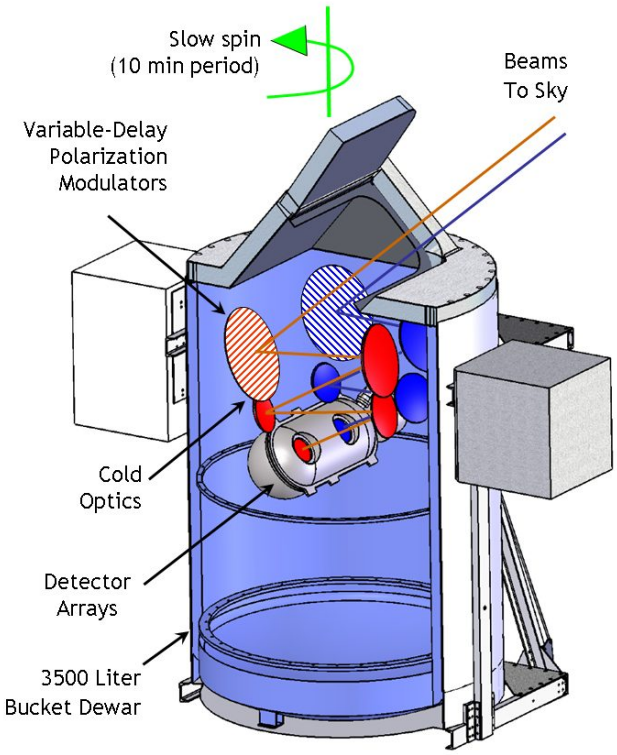

Figure 3. PIPER payload showing the twin telescopes mounted inside an open 3500 liter liquid helium dewar. Variable-delay polarization modulators provide simultaneous sensitivity to both linear and circular polarization. Four 32×40 arrays of transition-edge superconducting bolometers operating at 100 mK provide instrumental polarization sensitivity of NEQ $\sim 2\ \mu\mathrm{K\ s}^{1/2}$.

(PIPER) combines 5120 superconducting detectors with rapid polarization modulation to measure both linear and circular polarization. A series of high-altitude balloon flights maps 85% of the sky in each of 4 frequency bands. PIPER has the sensitivity, frequency coverage, and control of systematic errors needed to detect the primordial signal, while the high sky coverage provides the angular response needed to unambiguously separate the cosmic signal from the lensing foreground. A series of eight flights provides sensitivity $r < 0.007$ at 95% confidence.

2. INSTRUMENT DESCRIPTION

The Primordial Inflation Polarization Explorer (PIPER) is a balloon-borne instrument to measure the distinctive signature of primordial inflation in the linear polarization of the cosmic microwave background. Figure 3 shows the PIPER instrument. It consists of two co-aligned telescopes cooled to 1.5 K and mounted within a large liquid helium bucket dewar. A variable-delay polarization modulator (VPM) on each telescope injects a phase delay between incident orthogonal linear polarizations, which are then re-combined and re-imaged onto a focal plane containing 5120 superconducting bolometers cooled to 100 mK.

2.1 Optics

PIPER uses fully cryogenic optics, with all optical surfaces maintained at 1.5 K or colder within a 3500 liter liquid helium bucket dewar. Boiloff helium gas maintains a cold barrier between the optics and the ambient atmosphere; there are no windows or other emissive elements between the telescope and the sky.

The fully cryogenic design provides two important advantages. The first is sensitivity. With no warm elements in the optical path, instrumental emission and associated photon noise are reduced to negligible levels. PIPER

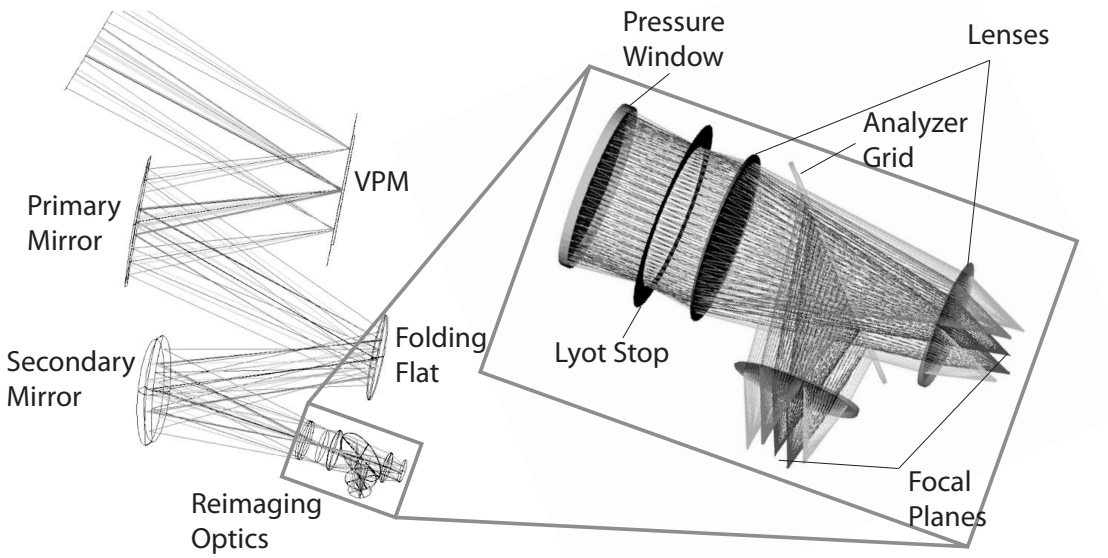

Figure 4. Ray trace analysis for a single PIPER telescope showing the VPM, reflective fore-optics, and reimaging optics within the detector cryostat. The cryogenic optics allow sufficient design flexibility to combine high performance within a compact footprint, producing Strehl ratio > 0.97 across the full $4.^{\circ}7 \times 6^{\circ}$ field of view on the sky.

operates within a few percent of the photon noise limit imposed by the atmosphere at balloon altitudes. The gain in sensitivity is significant: PIPER is a factor of three more sensitive than a comparable instrument with ambient-temperature (250 K) optics. The improved sensitivity in turn provides an order-of-magnitude decrease in integration time, allowing PIPER to reach noise levels in a single overnight flight that would otherwise require a week or more of integration from a long-duration Antarctic flight. Overnight observations are highly desirable: freed from restrictions on pointing too close to the Sun, PIPER can observe nearly 2π steradians in a single flight to measure the B-mode signal across the "reionization bump."

The second principal advantage of cryogenic optics is flexibility for the optical design. With no noise penalty for additional reflecting surfaces, the optical path can be optimized for throughput and beam quality. Figure 4 shows the optical design. Light from the sky enters a windowless liquid helium bucket dewar and reflects from a variable-delay polarization modulator (§2.2), which creates a phase delay between orthogonal linear polarization states incident on the telescope. Reflective fore-optics consisting of a primary mirror, folding flat, and secondary mirror transfer the light to reimaging optics within the detector cryostat.

The near-Gregorian fore-optics on each telescope reimage the primary pupil (at the VPM) to the secondary pupil within the detector cryostat. A Lyot stop at the secondary pupil controls illumination on the VPM. An anti-reflection coated silicon lens then slows the beam before it passes through a analyzer grid which splits the recombined beam into two orthogonal linear components. Each polarization passes through a final lens that converts the beam to f/1.6 before illuminating one of two identical total-power detector arrays.

PIPER achieves excellent optical performance in a compact configuration. Strehl ratios vary from 0.99 to 0.97 across each 32×40 pixel detector array. Despite the off-axis fore-optics, the beams on the sky are highly symmetric across the full $4.^{\circ}7 \times 6^{\circ}$ field of view on the sky.[13]

2.2 Polarization Modulation

Variable-delay polarization modulators impose a fast (3 Hz) modulation on the polarized component of the incident light to allow efficient detection of faint polarized signals in the presence of much brighter unpolarized emission.[14–16] Figure 5 shows the design. Each VPM consists of a regular grid of 41 μm diameter wires spaced 112 μm apart in front of a flat reflective plate. Incident light polarized parallel to the wires reflects from the grid. The perpendicular component is transmitted through the grid to the reflective backshort and back

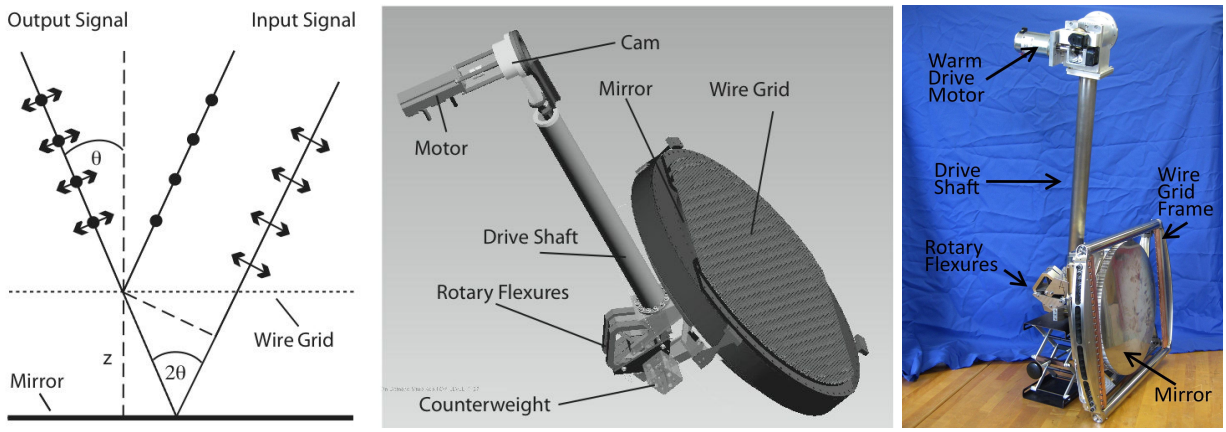

Figure 5. (Left) Schematic of VPM operation. The VPM uses a wire grid positioned in front of and parallel to a moving flat mirror. The phase delay between orthogonal linear polarizations is controlled by modulating the grid–mirror separation. (Right) CAD model of the VPM. A warm motor and cam connect to the cryogenic section to move the mirror. A rotary flexure maintains parallelism between the mirror and grid. (Right) VPM assembly prior to wire grid installation. The entire structure is made from stainless steel to minimize displacement or distortion from differential thermal contraction during cryogenic operation.

through the grid again, where it recombines with the parallel component. The additional distance traveled by the perpendicular component creates a phase delay between the components in the recombined beam. In the limit that the wavelength is large compared to the wire geometry, the phase delay may be written

$$\phi = \frac{4\pi z}{\lambda} \cos\theta \tag{2}$$

where z is the separation between the grid and the backshort, λ is the observing wavelength, and θ is the angle of incidence*. The recombined beams pass through a second analyzer grid with wires oriented at 45° with respect to the VPM grid. The reflected and transmitted components are orthogonal linear combinations of the polarization states defined by the VPM grid. Defining a coordinate system such that Stokes U is parallel to the VPM wires, the power incident on the detector arrays following the analyzer grid may be written

$$\begin{aligned} P_R &= 1/2\,[I + Q\cos\phi - V\sin\phi] \\ P_T &= 1/2\,[I - Q\cos\phi + V\sin\phi]\ , \end{aligned} \tag{3}$$

where P_R and P_T refer to the reflected and transmitted legs, respectively.[17] As the VPM backshort sweeps back and forth, the power incident on each detector consists of a dc term (Stokes I) plus modulated terms proportional to the linear (Q) and circular (V) polarization.

Each telescope has a VPM as the first element in the optical path to modulate the sky signal prior to injection of any elliptical polarization from the reflective optics. Each VPM modulates Stokes Q in a coordinate system defined by the orientation of the wires in the reflective grid. The two telescopes orient the VPM grid wires at 45° to each other so that one VPM is sensitive to Stokes Q and the other to Stokes U in a coordinate system fixed on the sky. Parallactic rotation of the sky relative to the instrument allows cross-calibration of the two telescopes.

The sensitivity to each polarization state depends on the VPM mirror stroke. A sinusoidal mirror stroke minimizes transient acceleration while providing sensitivity to both linear and circular polarization. We stroke the mirror through linear translation $\Delta z \approx 0.3\lambda$ to sample both the $-Q$ and $+Q$ peaks of the detector response (Eq. 3). The resulting modulation provides effective sensitivity of 0.75 for linear polarization and 0.62 for circular polarization relative to an ideal (square-wave) stroke.

*This equation sometimes appears in the literature with the $\cos\theta$ factor incorrectly placed in the denominator. This treatment is correct.

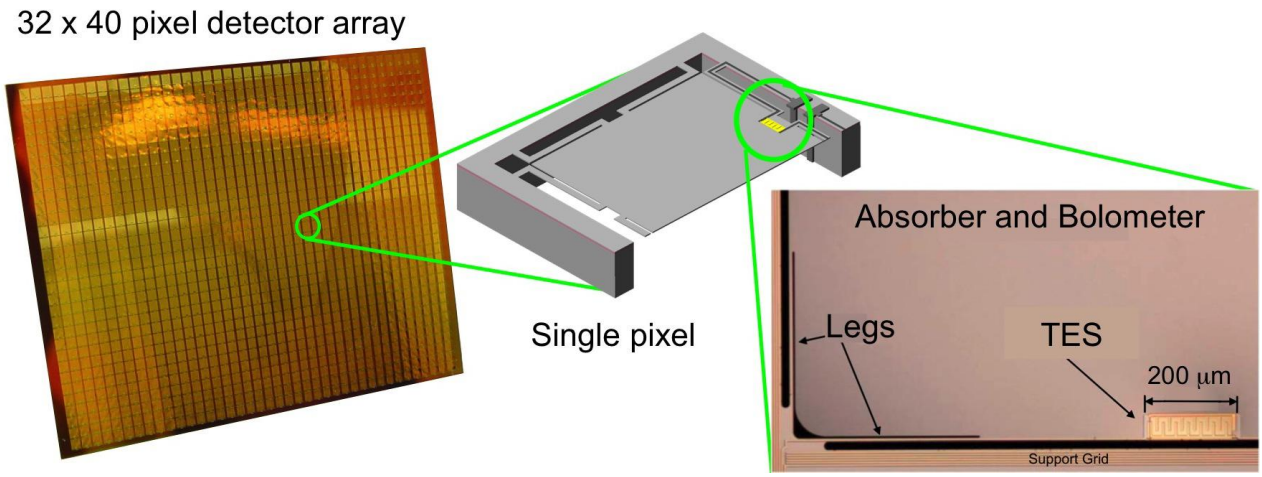

Figure 6. Detector arrays. (Left) Fabricated 32×40 prototype array with absorbing grid. (Center) Schematic showing backshort-under-grid architecture for a single pixel. (Right) Photomicrograph showing transition-edge superconducting bolometer and the supporting legs.

2.3 Detectors

The phase-delayed, re-combined beams from the VPM and optical system within each telescope are split by an analyzer grid and imaged onto total-power detector arrays. PIPER uses four identical 32×40 pixel arrays (one in each linear polarization for each of two telescopes) for a total of 5120 detectors within the instrument.

Figure 6 shows the PIPER detector array. PIPER uses transition-edge superconducting (TES) bolometers formed from a Mo:Au bilayer with normal-state resistance 20 mΩ. Interdigitated normal metal stripes suppress noise.[18] The bolometers are located on a square silicon membrane 1.4 μm thick mounted in planar array using the Backshort-Under-Grid (BUG) architecture[19] with pixel pitch 1135 μm. A reflective backshort behind each pixel increases the electric field intensity near the membrane to increase detector absorption. The fixed backshort distance is chosen to maximize absorption in the lowest three PIPER bands containing appreciable CMB signal while reducing absorption in the highest frequency band to prevent saturation from the bright dust signal.

The BUG architecture allows efficient coupling to the sky. The sky is imaged directly onto the detector array; there are no feed horns or similar coupling structures. A deposited bismuth layer on the suspended membranes provides impedance matching to free space. Electrical patches deposited on the grid walls carry signals from the bolometers to the back surface of the array; there are no reflective traces on the sky side of the array. The detector array mates directly to a NIST two-dimensional time-domain multiplexer chip using indium bump-bond technology.[20] The detectors are read out using the University of British Columbia Multi-Channel Electronics (MCE).[21]

3. SYSTEMATIC ERRORS

Measurement of a small linear polarization in the presence of much brighter unpolarized sources requires careful control of systematic error. The PIPER design avoids several potential effects entirely while reducing others to negligible levels.

3.1 $T \longrightarrow B$

The mixing of unpolarized flux into a false polarized signal, commonly referred to as "instrumental polarization," is especially important to control given that the unpolarized flux is likely to be a factor of 10^8 larger than the B-mode signal. Scattering, off-axis reflections, and transmission through dielectrics can all induce polarization on an initially unpolarized signal. PIPER's VPMs are placed at the front of the optical system so that the polarization modulation is encoded on the CMB before any of these effects can occur within the instrument.

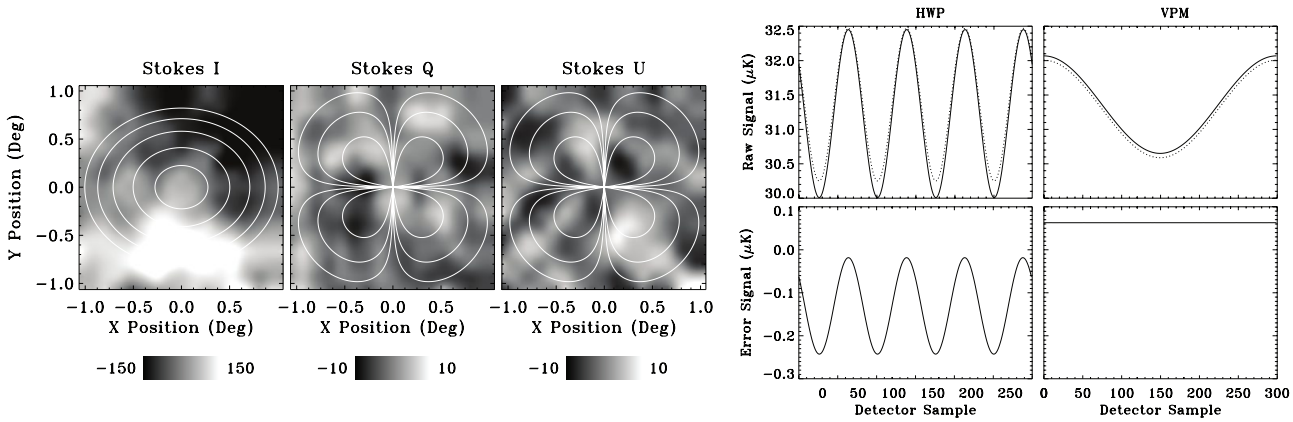

Figure 7. (LEFT) Simulated sky maps for I, Q, and U are shown with co-polar and cross-polar beams superposed. The cross-polar level assumed is -25 dB. Angular rotation of the cross-polar response relative to the linearly polarized sky signal produces a systematic error signal mixing Stokes Q and U. (RIGHT) Time-ordered signals for a half-wave plate and VPM modulation. The upper panels show the simulated signals with (dashed) and without (solid) the cross-polar response, while the bottom panels show the difference between the two cases.

The symmetric instrument design mitigates any residual effects resulting from imperfections in the VPM. Each VPM feeds two detector arrays which sense orthogonal linear combinations of the Stokes Q and V parameters (Eq. 3). Sky signals have opposite signs in the two arrays, while instrumental effects (differential emissivity, etc) produce the same sign in both arrays.

Fully cryogenic operation further mitigates instrumental polarization. Radiation scattered or diffracted from the VPM or other optical surfaces terminates within an absorbing cavity inside the bucket dewar. Superfluid liquid helium forces the cavity to be isothermal to mK precision, eliminating temperature gradients within the 1.5 K instrument stage. Gradients can exist within the 100 mK stage, but surfaces at this temperature have negligible mm-wave emission.

3.2 $\Delta T \longrightarrow B$

Instrument asymmetry can alias unpolarized temperature fluctuations on the sky into a false polarization signal. Front-end VPM modulation mitigates this effect by injecting a time-dependent phase delay between orthogonal polarizations without altering the beam shape on the sky. The 3 Hz modulation is rapid compared to the scan motion of the beam across the sky: PIPER does not rely on pixel-to-pixel comparisons for determination of the sky polarization.

3.3 $E \longrightarrow B$

B-mode polarization is faint compared to the dominant E-mode signal. Instrumental mixing of Stokes Q and U produces a similar mixing of E and B, potentially masking the primordial B-mode signal behind a brighter systematic error. PIPER takes advantage of the difference between astrophysical linear and circular polarization to eliminate this source of error. The VPM modulates the instrument response between linear polarization (Stokes Q) and circular polarization (Stokes V). The sky at millimeter wavelengths contains multiple sources of linear polarization but no significant circular polarization: the Stokes V signal from the sky should be negligible. Instrumental effects (e.g. a cross-polar beam response) combine with the VPM modulation to map linearly polarized sky signals into a false V signal. However, with no sky V signal to serve as a source, there is no corresponding mapping of sky V into a false Q signal and hence no mixing of Q and U.

Figure 7 illustrates the VPM advantage. Typical beam patterns yield cross-polar response at the -25 dB level. Rotation of the cross-polar beam pattern with respect to the sky (either from physical rotation of the instrument or rotation of the polarization basis by a half-wave plate) mixes Stokes Q and U to yield an error signal indistinguishable from true sky polarization. The VPM, in contrast, rotates between linear and circular

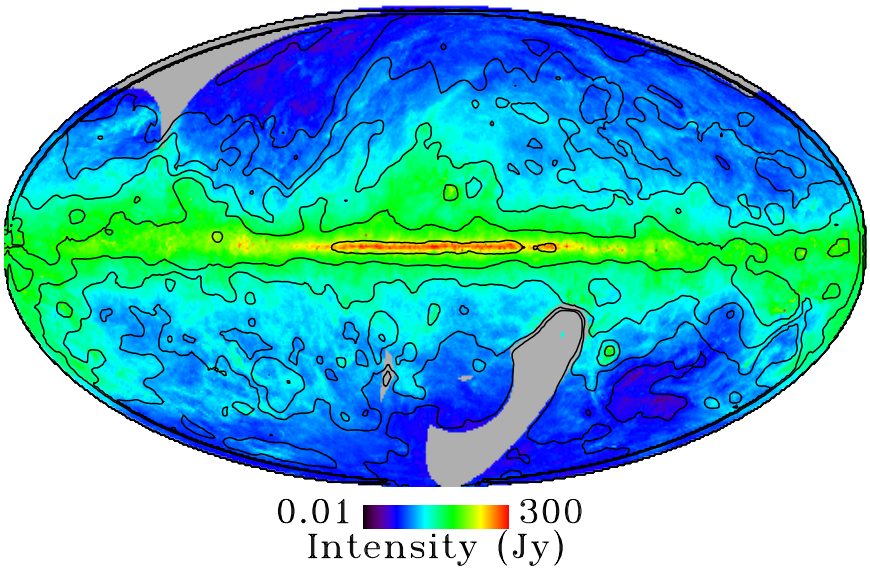

Figure 8. PIPER sensitivity and sky coverage. The map shows the polarized dust intensity at wavelength 500 microns. assuming a constant 3% dust fractional polarization. Contours show signal-to-noise ratio 3, 10, 30, 100, and 1000 within each beam spot on the sky. Overnight flights from Ft Sumner, NM and Alice Springs, Australia combine to observe the diffuse polarized emission at high signal to noise ratio over 85% of the sky.

polarization. Since the sky contains no significant circular polarization, the error signal is negligible (see, e.g., Ref [22] Appendix A for a discussion of VPM cross-polar response).

4. FLIGHT OPERATIONS

PIPER operates as a conventional balloon payload launched from mid-latitude sites. The focal plane images a $4.^{\circ}7 \times 6^{\circ}$ field of view on the sky pointed 50° from vertical. During the day the payload scans in azimuth to map selected regions of the sky in the anti-solar direction, providing deep integrations over small regions of the sky. During the night the payload spins about a vertical axis once every 10 minutes to rapidly map large areas of the sky. A single overnight flight observes more than 50% of the sky. We anticipate a series of flights alternating between northern and southern hemisphere sites to maximize sky coverage (Figure 8).

PIPER will map the sky in both linear and circular polarization (Eq. 3). At millimeter wavelengths, the sky is expected to have negligible circular polarization. Maps of the circular polarization thus provide an independent realization of the noise as well as a test for systematic errors.

The high sky coverage allows PIPER to measure the expected rise in B-mode power at $\ell < 10$ (the "reionization bump") where the primordial signal may best be distinguished from the lensing foreground. The first flight is currently scheduled for September 2013 from Ft Sumner, NM.

REFERENCES

1. V. A. Rubakov, M. V. Sazhin, and A. V. Veryaskin, "Graviton creation in the inflationary universe and the grand unification scale," *Physics Letters B* **115**, pp. 189–192, Sept. 1982.
2. R. Fabbri and M. D. Pollock, "The effect of primordially produced gravitons upon the anisotropy of the cosmological microwave background radiation," *Physics Letters B* **125**, pp. 445–448, June 1983.
3. L. F. Abbott and M. B. Wise, "Constraints on generalized inflationary cosmologies," *Nuclear Physics B* **244**, pp. 541–548, Oct. 1984.
4. A. G. Polnarev, "Polarization and anisotropy induced in the microwave background by cosmological gravitational waves," *Astronomicheskii Zhurnal* **62**, pp. 1041–1052, Dec. 1985.

5. R. L. Davis, H. M. Hodges, G. F. Smoot, P. J. Steinhardt, and M. S. Turner, "Cosmic microwave background probes models of inflation," *Physical Review Letters* **69**, pp. 1856–1859, Sept. 1992.
6. L. P. Grishchuk, "Cosmological perturbations of quantum-mechanical origin and anisotropy of the microwave background," *Physical Review Letters* **70**, pp. 2371–2374, Apr. 1993.
7. M. Kamionkowski, A. Kosowsky, and A. Stebbins, "Statistics of cosmic microwave background polarization," *Physcal Review D* **55**, pp. 7368–7388, June 1997.
8. U. Seljak and M. Zaldarriaga, "Signature of Gravity Waves in the Polarization of the Microwave Background," *Physical Review Letters* **78**, pp. 2054–2057, Mar. 1997.
9. E. Komatsu, J. Dunkley, M. R. Nolta, C. L. Bennett, B. Gold, G. Hinshaw, N. Jarosik, D. Larson, M. Limon, L. Page, D. N. Spergel, M. Halpern, R. S. Hill, A. Kogut, S. S. Meyer, G. S. Tucker, J. L. Weiland, E. Wollack, and E. L. Wright, "Five-Year Wilkinson Microwave Anisotropy Probe Observations: Cosmological Interpretation," *Astrophysical Journal Supplement Series* **180**, pp. 330–376, Feb. 2009.
10. J. Bock, S. Church, M. Devlin, G. Hinshaw, A. Lange, A. Lee, L. Page, B. Partridge, J. Ruhl, M. Tegmark, P. Timbie, R. Weiss, B. Winstein, and M. Zaldarriaga, "Task Force on Cosmic Microwave Background Research," *ArXiv Astrophysics e-prints* , Apr. 2006.
11. J. Dunkley, A. Amblard, C. Baccigalupi, M. Betoule, D. Chuss, A. Cooray, J. Delabrouille, C. Dickinson, G. Dobler, J. Dotson, H. K. Eriksen, D. Finkbeiner, D. Fixsen, P. Fosalba, A. Fraisse, C. Hirata, A. Kogut, J. Kristiansen, C. Lawrence, A. M. Magalha˜Es, M. A. Miville-Deschenes, S. Meyer, A. Miller, S. K. Naess, L. Page, H. V. Peiris, N. Phillips, E. Pierpaoli, G. Rocha, J. E. Vaillancourt, and L. Verde, "Prospects for polarized foreground removal," in *American Institute of Physics Conference Series*, S. Dodelson, D. Baumann, A. Cooray, J. Dunkley, A. Fraisse, M. G. Jackson, A. Kogut, L. Krauss, M. Zaldarriaga, & K. Smith , ed., *American Institute of Physics Conference Series* **1141**, pp. 222–264, June 2009.
12. Dodelson, S., et al., "The Origin of the Universe as Revealed Through the Polarization of the Cosmic Microwave Background," in *astro2010: The Astronomy and Astrophysics Decadal Survey*, *Astronomy* **2010**, pp. 67–+, 2009.
13. J. R. Eimer, P. A. R. Ade, D. J. Benford, C. L. Bennett, D. T. Chuss, D. J. Fixsen, A. J. Kogut, P. Mirel, C. E. Tucker, G. M. Voellmer, and E. J. Wollack, "The Primordial Inflation Polarization Explorer (PIPER): optical design," in *Society of Photo-Optical Instrumentation Engineers (SPIE) Conference Series*, *Society of Photo-Optical Instrumentation Engineers (SPIE) Conference Series* **7733**, July 2010.
14. D. T. Chuss, E. J. Wollack, S. H. Moseley, and G. Novak, "Interferometric polarization control," *Applied Optics* **45**, pp. 5107–5117, July 2006.
15. M. Krejny, D. Chuss, C. D. D'Aubigny, D. Golish, M. Houde, H. Hui, C. Kulesa, R. F. Loewenstein, S. H. Moseley, G. Novak, G. Voellmer, C. Walker, and E. Wollack, "The Hertz/VPM polarimeter: design and first light observations," *Applied Optics* **47**, p. 4429, Aug. 2008.
16. P. A. R. Ade, D. T. Chuss, S. Hanany, V. Haynes, B. G. Keating, A. Kogut, J. E. Ruhl, G. Pisano, G. Savini, and E. J. Wollack, "Polarization modulators for CMBPol," *Journal of Physics Conference Series* **155**, p. 012006, Mar. 2009.
17. D. T. Chuss, E. J. Wollack, R. Henry, H. Hui, A. J. Juarez, M. Krejny, S. H. Moseley, and G. Novak, "Properties of a variable-delay polarization modulator," *Applied Optics* **51**, p. 197, Jan. 2012.
18. J. G. Staguhn, C. A. Allen, D. J. Benford, J. A. Chervenak, M. M. Freund, S. A. Khan, A. S. Kutyrev, S. H. Moseley, R. A. Shafer, S. Deiker, E. N. Grossman, G. C. Hilton, K. D. Irwin, J. M. Martinis, S. W. Nam, D. A. Rudman, and D. A. Wollman, "TES detector noise limited readout using SQUID multiplexers," *Low Temperature Detectors* **605**, pp. 321–324, Feb. 2002.
19. C. A. Allen, D. J. Benford, J. A. Chervenak, D. T. Chuss, T. M. Miller, S. H. Moseley, J. G. Staguhn, and E. J. Wollack, "Backshort-Under-Grid arrays for infrared astronomy," *Nuclear Instruments and Methods in Physics Research A* **559**, pp. 522–524, Apr. 2006.
20. T. M. Miller, N. Costen, and C. Allen, "Indium Hybridization of Large Format TES Bolometer Arrays to Readout Multiplexers for Far-Infrared Astronomy," *Journal of Low Temperature Physics* **151**, pp. 483–488, Apr. 2008.

21. E. S. Battistelli, M. Amiri, B. Burger, M. Halpern, S. Knotek, M. Ellis, X. Gao, D. Kelly, M. Macintosh, K. Irwin, and C. Reintsema, "Functional Description of Read-out Electronics for Time-Domain Multiplexed Bolometers for Millimeter and Sub-millimeter Astronomy," *Journal of Low Temperature Physics* **151**, pp. 908–914, May 2008.
22. D. T. Chuss, P. A. R. Ade, D. J. Benford, C. L. Bennett, J. L. Dotson, J. R. Eimer, D. J. Fixsen, M. Halpern, G. Hilton, J. Hinderks, G. Hinshaw, K. Irwin, M. L. Jackson, M. A. Jah, N. Jethava, C. Jhabvala, A. J. Kogut, L. Lowe, N. McCullagh, T. Miller, P. Mirel, S. H. Moseley, S. Rodriguez, K. Rostem, E. Sharp, J. G. Staguhn, C. E. Tucker, G. M. Voellmer, E. J. Wollack, and L. Zeng, "The Primordial Inflation Polarization Explorer (PIPER)," in *Society of Photo-Optical Instrumentation Engineers (SPIE) Conference Series*, *Society of Photo-Optical Instrumentation Engineers (SPIE) Conference Series* **7741**, July 2010.